GaN *m*-plane: Atomic structure, surface bands, and optical response

M. Landmann,[1] E. Rauls,[1] W. G. Schmidt,[1] M. D. Neumann,[2] E. Speiser,[2] and N. Esser[2]
[1]*Lehrstuhl für Theoretische Physik, Universität Paderborn, 33095 Paderborn, Germany*
[2]*Leibniz-Institut für Analytische Wissenschaften-ISAS e.V., Schwarzschildstrasse 9, 12489 Berlin, Germany*
(Received 7 October 2014; published 7 January 2015)

Density-functional-theory calculations are combined with many-body perturbation theory in order to elucidate the geometry, electronic, and optical properties of the wz-GaN($1\bar{1}00$) surface, i.e., the so-called m-plane. The optical absorption and reflection anisotropy related to electronic transitions between surface states are identified by comparison with measured data covering transition energies from 2.4 up to 5.4 eV. Our results show a surface relaxation mechanism consistent with the electron counting rule that causes a moderate buckling of the GaN surface dimers and gives rise to two distinct surface states: The doubly occupied N dangling bonds form a surface band that is resonant with the GaN valence-band edge at the center of the Brillouin zone, whereas the empty Ga dangling bonds occur within the GaN band gap closely following the dispersion of the conduction-band edge. These two states contribute strongly to the formation of surface excitons that redshift the optical absorption with respect to the bulk optical response. The surface optical absorption i.e., the excitonic onset below the bulk band gap followed by a broad absorption band at higher energies related to the dispersion of the surface band structure, is calculated in agreement with the experimental data.

DOI: 10.1103/PhysRevB.91.035302 PACS number(s): 73.20.At, 68.35.B−, 78.40.Fy

I. INTRODUCTION

Gallium-nitride-based heterostructures have been routinely used since the 1990s for electronic and optoelectronic applications [1] that exploit its wide band gap of approximately 3.4 eV at room temperature. The low sensitivity of the material to ionizing radiation as well as its functionality at high temperatures and high voltages make it attractive for various electronic devices. Typically these devices are based on heterostructures grown on c-plane substrates; see Fig. 1 for the illustration of the most relevant low-index GaN crystal-surface planes. This orientation, however, gives rise to strong electric fields in the wurtzite material [2] that are often disadvantageous for the performance of devices. It has been demonstrated, however, that the epitaxial growth in a nonpolar direction allows the fabrication of structures free of electrostatic fields [3]. For this reason, in addition to the common c-plane, the nonpolar GaN surfaces, i.e., the m-plane with ($1\bar{1}00$) and the a-plane with ($11\bar{2}0$) orientation, are also of increasing interest. Both surfaces may contain an equal number of threefold-coordinated Ga and N in the top atomic layer, thus allowing charge neutrality to be obtained without changes in stoichiometry or reconstruction.

However, despite the well-defined and simple atomic structure of the m-plane surface, its electronic properties have been controversially discussed for years. Density functional calculations within the local density approximation (DFT-LDA) by Northrup and Neugebauer [4] predicted the stoichiometric surface structure, shown in Fig. 1, to be stable for almost any value of the Ga chemical potential and found a relaxation mechanism reminiscent of conventional III-V(110) surfaces: The cation changes its hybridization from a pure sp^3-type to a sp^2-like configuration, which was found to lead to a surface-layer buckling of about 7° with the N (Ga) moving out (in) by 0.02 Å (0.20 Å), as indicated in Fig. 1. The electronic structure calculations of Ref. [4] allowed the identification of two surface states. An occupied surface state is derived from surface N-2p orbitals, while the unoccupied surface state corresponds to Ga-localized dangling bonds. The moderate atomic relaxation of the surface layer increases the gap between these states by more than 1 eV such that for the fully relaxed structure, the N-derived band lies just below the valence-band maximum (VBM), while the Ga-derived band lies just above the conduction-band minimum (CBM). Thus, according to these DFT-LDA calculations, there should be no intrinsic surface states in the fundamental gap of the GaN m-plane [4].

This contrasts with DFT calculations by Segev and Van de Walle [5,6]. They used particularly modified pseudopotentials in order to cope with the DFT band-gap underestimation and predicted an unoccupied Ga-dangling-bond state at ∼0.7 eV below the CBM for the GaN m-plane. The occupied surface band, according to Refs. [5,6], is associated with dangling bonds on the N atoms and overlaps energetically with the bulk valence band, i.e., it does not create levels within the band gap. Consistent with the picture by Northrup and Neugebauer, but deviating from the results by Segev and Van de Walle, more recent DFT-LDA calculations [7] predict the doubly degenerate N-derived highest-occupied and Ga-derived lowest-unoccupied surface states to be energetically degenerate with the corresponding bulk band edges.

Interestingly, the most recent calculations on that system known to us come to a different conclusion: The LDA + U approach by Lymperakis *et al.* [8] yields a Ga-derived surface state that is in the whole Brillouin zone in the fundamental band gap of GaN and never resonant with the bulk bands. Thus, the theoretical studies on the GaN m-plane agree on the relaxation mechanism and orbital character of surface states, but differ appreciably concerning the energy position of the unoccupied surface state with respect to the bulk band edge.

Experimentally, there are also contradicting reports on the existence of empty surface states in the GaN bulk band gap. From earlier scanning tunneling microscopy and spectroscopy (STM and STS, respectively) data on the GaN m-plane surface [7,9], it was concluded that both the N and Ga dangling-bond

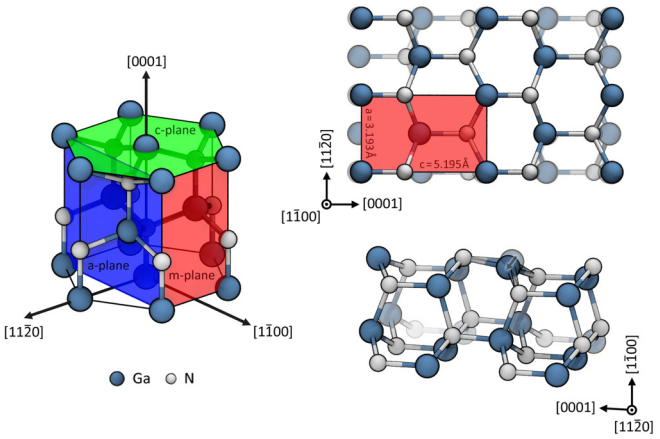

FIG. 1. (Color online) Left: Conventional unit-cell representation of wz-GaN bulk material including the definition of the most relevant low-index crystal-surface planes. The polar c-plane and the two nonpolar m- and a-planes are shown in green, red, and blue, respectively. Right: Atomic structure of the relaxed GaN m-plane surface shown as top view, including the definition of the surface unit cell (top), and side view indicating the surface relaxation mechanism (bottom). Atoms within (below) the topmost atomic double layers are shown in full (translucent) color in the top view.

states are outside of the fundamental gap, while the most recent data obtained with high resolution [8] yield a different picture. The debated empty surface state was found well below the conduction-band minimum within the fundamental band gap, but with a very low density of states due to its dispersion characteristics. According to Ref. [8], the GaN m-plane is intrinsically pinned at around 0.6 eV below the CBM. The shrinkage of the GaN bulk band gap due to the occurrence of surface states agrees with recent reflection anisotropy spectroscopy (RAS) data [10], which have shown surface optical transitions around 3.3 eV, i.e., below the GaN bulk band gap at 3.4 eV, attributed to gap states.

In the present study, we aim to clarify the electronic properties of the GaN m-plane. Thereby, we go methodologically beyond previous theoretical studies by performing hybrid functional in addition to (semi)local functional DFT calculations and include many-body effects in the surface optical response on the Bethe-Salpeter equation (BSE) level of theory. Our results show a strong sensitivity with respect to the slab size and demonstrate the existence of bound Ga-derived surface states just below the CBM. Moreover, we address the surface optical response experimentally and detect optical absorption related to surface electronic states. In particular, a surface excitonic absorption at an energy below the bulk absorption onset is found, accompanied by a broad spectral feature that extends to higher energies, which is related to the dispersion of the two surface bands.

II. METHODOLOGY AND NUMERICAL DETAILS

The present calculations are performed using density functional theory (DFT) within the generalized gradient approximation (GGA) to the electron exchange and correlation (XC) as well as using hybrid functional DFT. Specifically, the Perdew-Burke-Ernzerhof (PBE) [11] and Heyd-Scuseria-Ernzerhof (HSE) functionals [12] were used for the GGA and hybrid functional calculations, respectively. In the latter, a 32% fraction of exact exchange (EXX) from Hartree-Fock theory was used. As previously demonstrated, the increased EXX fraction accurately reproduces features of the GW quasiparticle band structure [13]. Additionally, self-energy–corrected (Ga_{3d} as well as N_{2p} states; for details see Ref. [13]) LDA-1/2 [14], and Hubbard-corrected PBE + U (corrections to Ga_{3d} and N_{2p} states) calculations were performed in order to compare various approaches to overcome the DFT band-gap problem [15]. The electron-ion interaction is described by the projector-augmented wave scheme [16], where the Ga $3d$ states are treated as valence electrons. The electronic wave functions are expanded into plane waves up to a kinetic energy of 400 eV. All calculations were performed using the Vienna *Ab initio* Simulation Package (VASP) [17].

The surface is modeled by periodically repeated symmetric slabs. Each supercell contains between 16 and 48 atomic layers as specified below, and a vacuum region equivalent to about 16 atomic layers (∼22 Å). The uppermost 4 (16) atomic layers on each side of the 16-layer (48-layer) slabs are allowed to relax until the forces on the atoms are below 0.001 meV/Å. The Brillouin-zone integration is performed using regular Γ-centered meshes with a **k**-point density of $16 \times 24 \times 1$ ($8 \times 12 \times 1$) for the 16 (48) atomic layers slab. The surface calculations were performed using the DFT-PBE equilibrium lattice constants of $a = 3.193$ Å and a c/a ratio of 1.627, which are close to the experimental values of $a = 3.189$ Å and $c/a = 1.626$ at room temperature [18]. In addition, these lattice parameters are very close to the DFT-HSE parameters $a = 3.198$ Å and $c/a = 1.627$ [19]. The deviation between calculated and measured lattice parameters changes the band-structure energies by less than 0.1 eV.

Starting from the DFT-PBE electronic structure but using the eigenvalues from the hybrid DFT, the optical response of GaN bulk and surface slabs has been calculated solving the Bethe-Salpeter equation for coupled electron-hole excitations [20–22]. It incorporates the screened electron-hole attraction as well as the unscreened electron-hole exchange. Specifically, we use the time-evolution method developed by one of the present authors [23,24] as well as an iterative diagonalization procedure [25] to obtain the polarizability. The deviations resulting from using the HSE eigenvalues rather than the GW quasiparticle energies in the BSE is found to be of the order of one tenth of an eV.

In contrast to zinc-blende or diamond-type semiconductors, GaN in the wurtzite crystal structure exhibits a pronounced bulk optical anisotropy which is superimposed onto the surface optical anisotropy. Recently, it has been demonstrated that by surface modification due to oxygen adsorption, the optical anisotropy is significantly changed, which has been interpreted in terms of quenching the surface optical response [10].

In the present study, the anisotropy of the optical response is simulated from the BSE dielectric functions in terms of a three-layer model and compared to experimental RAS data. Compared to previous experimental results [10], the RAS measurements have been extended to a broader energy window between 2.4 and 5.4 eV.

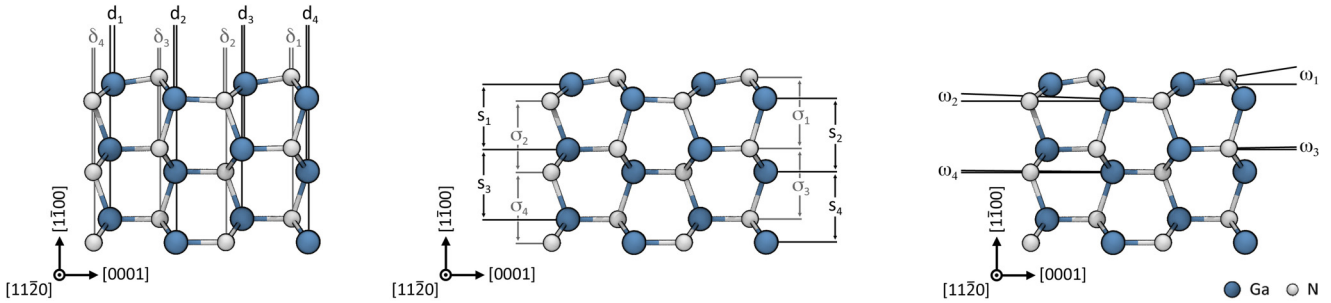

FIG. 2. (Color online) Definition of characteristic structural relaxation parameters for the GaN m-plane. Left: Lateral displacement parameters d_i and δ_i defined along the [0001] surface direction for the Ga and N sublattices. Middle: Interlayer spacing parameters s_i and σ_i defined separately for interatomic distances along the [1$\bar{1}$00] surface normal for the Ga and N sublattices. Right: Buckling parameters ω_i describing the tilting of Ga-N dimers with respect to the surface plane. The parameters are defined for the topmost four layers ($i = 1,2,3,4$) with respect to the DFT optimized atom positions.

In contrast to optically isotropic materials such as zinc-blende or diamond-type semiconductors, the often used thin-layer approximation of an anisotropic surface layer on an isotropic substrate (bulk) [26,27] is no longer valid. Instead the sample is modeled as an optically uniaxial slab with finite thickness on top of an optically uniaxial film in an isotropic ambient, using the expressions for the reflection by stratified planar structures [28]. Thereby, the calculated optical response, i.e., the dielectric functions (DFs) of slab and bulk and the slab thickness, are used as input parameters. In order to account for the influence of the two sides of the slab on the calculated DF, the imaginary part of the DF is divided by two and an effective film thickness of 11 Å is used. Since the RAS experiments are performed near normal incidence, the sensitivity to the out-of-plane component of the DF is negligible.

III. RESULTS AND DISCUSSION

A. Surface relaxation

The side view of the structurally relaxed GaN m-plane is shown in Fig. 2, with the calculated values for key structural parameters obtained within either local or hybrid DFT summarized in Table I. The relaxed geometry calculated here agrees with previous calculations, e.g., Refs. [4,5], which find a moderate buckling in the uppermost atomic layer with the surface N (Ga) atoms moving out (in) with respect to their bulk positions. The buckling angle in the uppermost layer of about 8° calculated here is similar to the value predicted in Ref. [4], where 7° is reported. Also the contraction of the Ga-N dimer length of about 7–8 % calculated here agrees with the value of 6 % determined in Ref. [4]. Interestingly, the geometry of the relaxed surface does not change considerably if hybrid functional rather than local DFT calculations are performed, with deviations even at the outermost atoms below 0.1 Å. Changes of similar magnitude are observed if the slab size is increased from 16 to 48 atomic layers. The present calculations thus suggest that the relaxation mechanism as well as the relaxation parameters are robust with respect to the treatment of the XC effects and that a 16-layer slab is sufficient to model the *structural* surface properties.

Northrup and Neugebauer [4] suggest that the structural relaxation is caused by a rehybridization of the surface N and Ga atoms towards a sp^3 and sp^2 configuration, respectively. This leads to a tilting of the GaN dimer because the sp^2 hybridized Ga prefers a planar bonding situation. This relaxation mechanism is well known from III-V(110) surfaces [29,30] and is consistent with electron counting heuristics [31]. The latter states that stable compound semiconductor surfaces are typically characterized by all the dangling bonds on the

TABLE I. Summary of structural relaxation parameters defined in Fig. 2 as well as Ga-N dimer-bond lengths b_i calculated within DFT-PBE and DFT-HSE. All lateral displacement and interlayer spacing parameters are given in Å. Buckling parameters are given in degree. Values in brackets are the percentage change with respect to the values in wz-GaN bulk.

	16 monolayers		48 monolayers
	DFT-PBE	DFT-HSE	DFT-PBE
d_1	0.145	0.150	0.129
d_2	−0.044	−0.030	−0.044
d_3	0.008	0.011	0.009
d_4	−0.017	−0.021	−0.023
δ_1	−0.015	−0.025	−0.023
δ_2	−0.040	−0.033	−0.049
δ_3	−0.002	−0.005	−0.003
δ_4	−0.011	−0.011	0.013
s_1	2.563 (−7.87)	2.514 (−9.07)	2.572 (−6.98)
s_2	2.871 (3.82)	2.839 (2.67)	2.859 (3.39)
s_3	2.741 (−0.86)	2.715 (−1.82)	2.742 (−0.83)
s_4	2.785 (0.70)	2.781 (0.58)	2.802 (1.34)
σ_1	2.789 (0.86)	2.710 (−2.00)	2.780 (0.54)
σ_2	2.800 (1.25)	2.777 (0.43)	2.798 (1.18)
σ_3	2.775 (0.51)	2.758 (−0.26)	2.787 (0.77)
σ_4	2.772 (0.24)	2.768 (0.10)	2.776 (0.38)
ω_1	8.34	7.63	8.01
ω_2	2.45	2.20	2.46
ω_3	1.12	1.28	1.35
ω_4	0.37	0.39	0.67
b_1	1.818 (−7.14)	1.800 (−8.08)	1.823 (−6.86)
b_2	1.963 (0.29)	1.956 (−0.08)	1.954 (−0.15)
b_3	1.948 (−0.48)	1.942 (−0.78)	1.946 (−0.59)
b_4	1.958 (0.31)	1.968 (0.50)	1.965 (0.37)

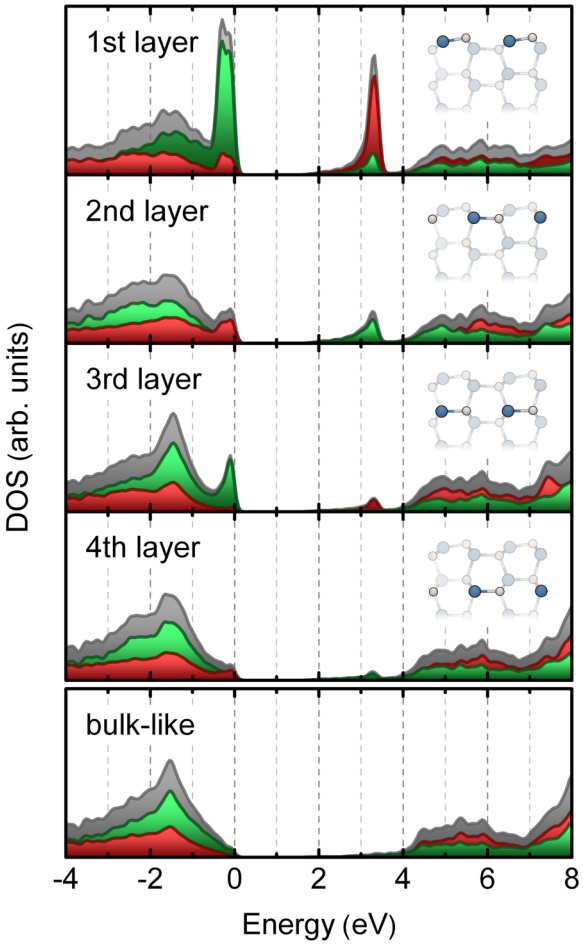

FIG. 3. (Color online) Layer-resolved total (gray shaded) as well as Ga (red) and N (green) projected contributions to the GaN 16-layer surface-slab DFT-PBE density of states. Insets: The atoms that have been considered in the projection of the density of states. The bulklike contributions in the lowermost panel originate from the average of the eight central atomic layers of the surface slab.

electronegative element occupied and all the dangling bonds on the electropositive element empty, given the number of available electrons [32,33]. In the present case, this implies a charge transfer from surface Ga to N. This charge transfer occurs indeed, as demonstrated in the layer-resolved and atomic projected electron density of states (DOS) given in Fig. 3. Obviously, the first-layer DOS deviates significantly from its bulk value in the sense that additional filled N states appear close to the VBM, while empty Ga states appear below the bulk CBM. This agrees nicely with the finding discussed above that the Ga atom assumes a more planar bonding configuration consistent with a moderate buckling of about 8°. However, as shown in Fig. 3, a similar, albeit far smaller, charge transfer from Ga to N occurs in the third layer, and gives rise to a buckling of about 1°. A slight accumulation of filled Ga states and empty N states close to the bulk VBM and CBM, however, occurs in the second and, to some extent, even in the fourth atomic layer. Accordingly, a buckling of opposite direction of about 2° and below 1° occurs in these layers. The DOS underneath the fourth atomic layer, finally, is reminiscent of the bulk characteristics in both 16- and 48-layer slabs.

B. Surface electronic band structure

In order to address the controversy on the precise position of the Ga and N surface states with respect to the GaN bulk band edges, we explore the surface band structure and compare the calculated and experimentally determined optical anisotropy. Data obtained within PBE for a 16-layer surface slab are shown in Fig. 4. Thereby, the alignment of the bulk and surface bands has been done using the average of the local electrostatic potentials [34]. Two bound surface states, i.e., one occupied and one unoccupied, occur in the GaN band gap. The filled surface state is energetically degenerate with the bulk VBM at the Γ point, but otherwise well separated from the continuum of bulk states. The empty surface states are below the bulk GaN conduction states throughout the surface Brillouin zone, and just below (PBE, 16-layer slab) or slightly underneath (see $\Delta E_{S_{\mathrm{Ga}}}$ in Table II) the bulk CBM at the Γ point. The orbital character of the respective states is shown in Fig. 5. It can be seen that the occupied surface state is mainly formed by N-2p orbitals from the uppermost surface anion, with minor contributions from the surface Ga atoms and second-layer N. The unoccupied surface state corresponds mainly to a surface Ga localized nonbonding p orbital, with minor contributions from the cations in the second, third, and fourth atomic layer. These findings corroborate the electron-counting rule driven relaxation mechanism discussed above as well as the early assignment by Northrup and Neugebauer [4]. The energy of the surface states, however, deviates somewhat from Ref. [4] where these were found to be resonant with bulk states at the bulk edges. On the other hand, the separation between the Ga-derived surface state and the bulk band edge calculated here is far smaller than predicted in Refs. [5,6,8].

In order to determine the precise position of the Ga-derived surface state, we investigate the influence of the slab size as well as of the approximation for electron XC effects. Lymperakis *et al.* [8] pointed out that slabs consisting of less than 24 layers do not contain enough bulklike material to correctly describe the onset of the bulk conduction band. Therefore, we perform additional calculations using 48-layer slabs. The corresponding results for the energy gap between the surface states as well as the position of the Ga-derived surface state are compared with the bulk band gap calculated using the same approximation in Table II. The table presents results obtained using local as well as hybrid XC functionals (PBE

TABLE II. Fundamental direct Γ-Γ band gaps of GaN($1\bar{1}00$) surface slabs as well as wz-GaN bulk material calculated on various levels of theory (see text). The parameter $\Delta E_{S_{\mathrm{Ga}}}$ quantifies the band position of the Ga dangling-bond-related state below the bulk CBM at the Γ point.

XC	Layers	$E_{\mathrm{gap}}^{\mathrm{surf}}$	$E_{\mathrm{gap}}^{\mathrm{bulk}}$	$\Delta E_{S_{\mathrm{Ga}}}$
PBE	16	1.73	1.89	0.07
	48	1.65	1.85	0.20
HSE	16	3.31	3.55	0.20
	48	3.31	3.58	0.27
LDA-1/2	16	3.03	3.53	0.09
	48	2.96	3.16	0.20
PBE + U	48	2.68	3.35	0.66

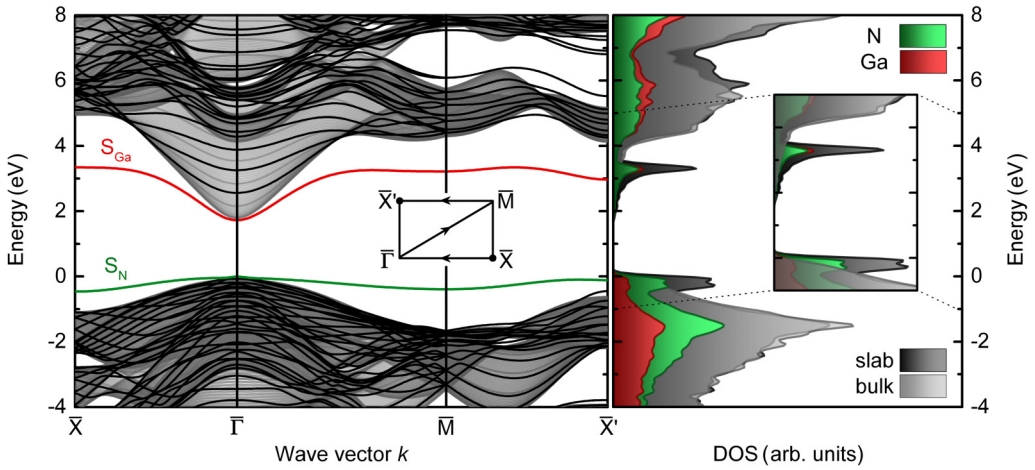

FIG. 4. (Color online) Left: DFT-PBE band structure (black lines) of the GaN m-plane 16-layer surface slab along high symmetry lines of the two-dimensional surface Brillouin zone (cf. inset). The Ga dangling-bond surface state S_{Ga} and the N dangling-bond surface-resonance state S_N derived energy bands are highlighted in red and green. The projection of the bulk electronic band structure is indicated in gray. Right: Total slab (dark-gray shaded) and wz-GaN bulk (light-gray shaded) densities of states as well as partial Ga (red) and N (green) projected surface-slab densities of states.

and HSE, respectively) in addition to LDA-1/2 and PBE + U results. The surface-state energy for the 16-layer slab has been determined from aligning the surface and bulk band structures by the microscopic average of the electrostatic potential. For 48-layer slabs, all band-energy differences, including the bulk band gap, have been extracted from the surface-slab eigenvalue spectrum. A direct comparison of the band structures and densities of states obtained for 16- and 48-layer surface slabs is shown in Fig. 6. Irrespective of the specific treatment of the XC effects, the usage of the ticker surface slab downshifts the energy of the Ga-derived surface state with respect to the bulk CBM. For the 48-layer slab, we obtain energy separations of 0.20, 0.27, and 0.20 eV within PBE, HSE, and LDA-1/2, respectively. The far-larger energy separation between the bulk conduction-band edge and the Ga surface state of 0.6 or 0.7 eV predicted on the basis of LDA + U calculations [8] or specifically designed pseudopotentials with additional repulsive contributions [5,6] are reproduced in the present work by PBE + U. The latter results in an energy separation of 0.66 eV. This value certainly marks the upper limit for the downshift of the empty surface state with respect to the bulk CBM. On the other hand, from the theoretical calculations, it appears clear that there is also a finite separation between empty bulk and surface states at Γ.

Experimentally, this separation has been doubted in early investigations [7,9]. This is easily understood from the low surface-state DOS compared to the bulk data, as can be seen in Figs. 4 and 6. Experimental hints for such a separation stem from highly resolved tunneling data [8], and in particular from measurements of the surface optical response [10].

C. Surface optical anisotropy

Based on the electronic structure above, the surface and bulk optical responses are calculated considering two-particle

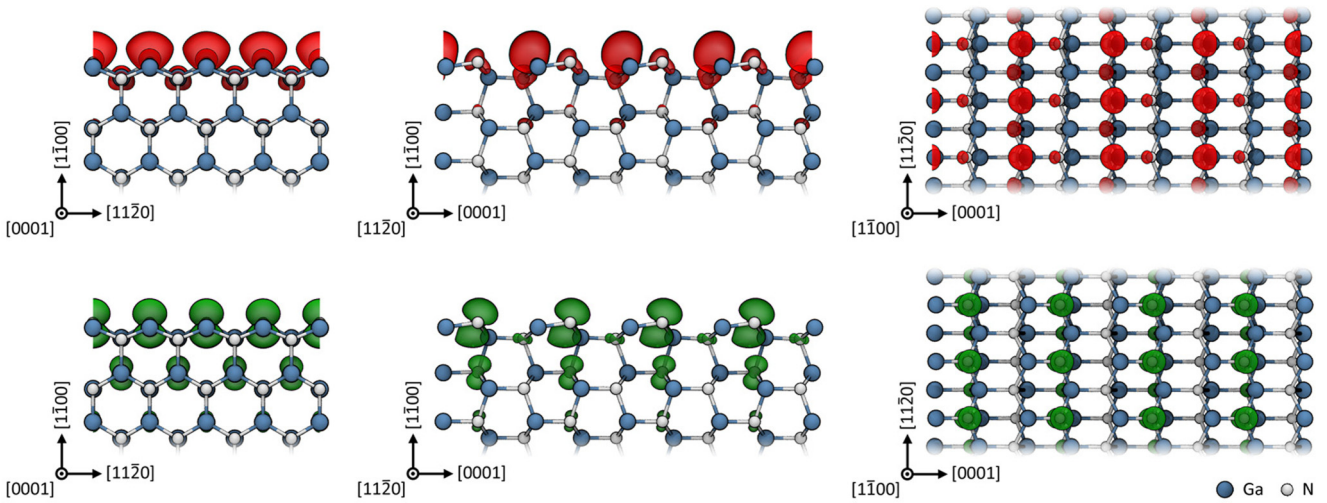

FIG. 5. (Color online) Visualization of the partial DFT-PBE charge densities (isovalue: 0.01 e/Å^3) of the surface state S_{Ga} (red) and the surface-resonance state S_N (green) (see Fig. 4) of the 16-layer surface slab along different viewing directions.

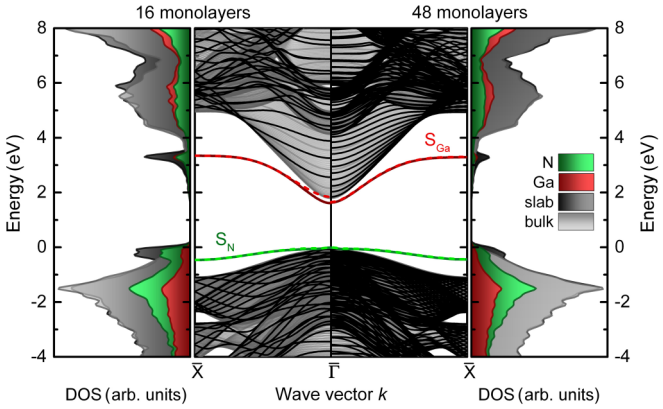

FIG. 6. (Color online) DFT-PBE band structure along the $\overline{\Gamma}$-$\overline{X}$ direction (black lines) as well as total (dark-gray shaded) and partial Ga (red) and N (green) densities of states for 16- (left) and 48-layer (right) surface slabs. The projection of the bulk electronic band structure along the $\overline{\Gamma}$-$\overline{X}$ surface direction is given in gray.

electron-hole excitations within the BSE formalism. The present calculations for the bulk optical response agree with earlier calculations [36,37] and closely resemble experimental findings obtained by spectroscopic ellipsometry of GaN($1\bar{1}00$) wurtzite-film samples at $T = 295$ K [35]; see Fig. 7. This holds in particular for the difference between the ordinary [$\varepsilon_2^{\perp}(\omega)$, light polarization perpendicular to the c direction] and extraordinary [$\varepsilon_2^{\parallel}(\omega)$, light polarization along c] dielectric function. The presence of an intrinsic surface state substantially influences the m-plane optical response. If one compares the results for GaN bulk and the 16-layer surface slab shown in Fig. 7, one sees that the onset of the optical response is redshifted with respect to the bulk data by about a few tenths of an eV. In particular, we find an enhanced optical anisotropy for low photon energies.

In order to quantify the contribution of the N and Ga surface states to the surface dielectric function, we perform additional calculations where the exciton Hamiltonian is set up from specific states only, and iteratively diagonalized. The contribution of surface-surface, surface-bulk, and bulk-bulk transitions to the total optical response of the 16-layer surface slab can thus be separately determined. The calculated data clearly show that electronic transitions between N- and Ga-derived surface states contribute to the total surface optical response at low photon energies; see top panel in Fig. 8. Thereby, the maximum of the ordinary and extraordinary dielectric function occurs at different energies, i.e., there is a clear surface-state-related contribution to the surface optical anisotropy.

However, exclusive transitions between the two surface states are not sufficient to model the onset of the surface dielectric function. The coupling to the unoccupied and occupied (cf. second and third panel in Fig. 8) bulklike bands of the slab is necessary in order to reproduce the low-energy part of the optical response. Moreover, in contrast to the low joint density of states at the Brillouin-zone center due to the particularly strong dispersion of Ga-derived surface band at $\overline{\Gamma}$, the surface optical absorption shows a pronounced peak associated with the onset of optical absorption in the ordinary

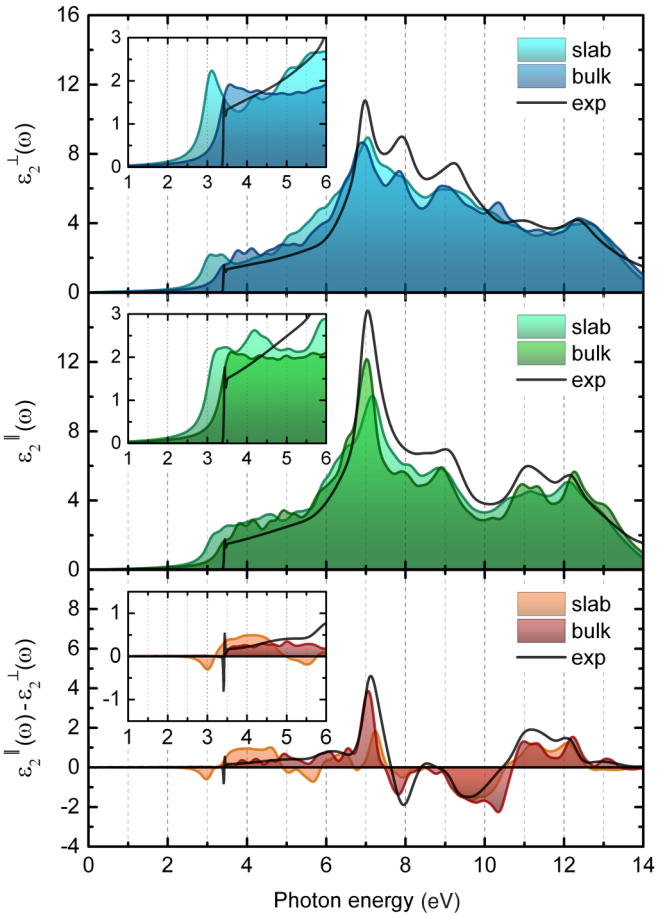

FIG. 7. (Color online) Polarization-dependent imaginary parts of the dielectric functions of the GaN m-plane surface slab and wz-GaN bulk material calculated on the BSE level of theory. The ordinary $\varepsilon_2^{\perp}(\omega)$ and extraordinary $\varepsilon_2^{\parallel}(\omega)$ imaginary components of the complex dielectric functions as well as the difference $\varepsilon_2^{\parallel}(\omega) - \varepsilon_2^{\perp}(\omega)$ are shown in the top, middle, and bottom panel, respectively. Black lines represent experimental data [35].

dielectric function. This indicates the formation of excitonic states at the GaN m-plane which extend into the subsurface layers. Consequently, N- and Ga-derived surface states as well as bulk states of the slab contribute to the surface exciton which defines the onset of the optical absorption of the m-plane.

It is also obvious from Fig. 8 that the lowest-unoccupied and highest-occupied surface bands give rise to characteristic features in the optical response: It shows a strong optical anisotropy related to very distinct absorption bands from above 3 eV, i.e., below the fundamental band gap, up to 5.5 eV. A narrow excitonic absorption in the calculated ordinary dielectric function occurs below the bulk band gap and a broad optical absorption band for higher energies in the extraordinary dielectric function. Consequently, the surface band-related optical absorption should give rise to a characteristic optical anisotropy. Indeed, this is observed experimentally. Figure9 shows RAS spectra obtained on clean GaN and after subsequent exposure to residual gas; see Ref. [10] for experimental details. There, photoelectron spectroscopy was used in conjunction with RAS to demonstrate that the change in optical anisotropy is due to the quenching of surface states.

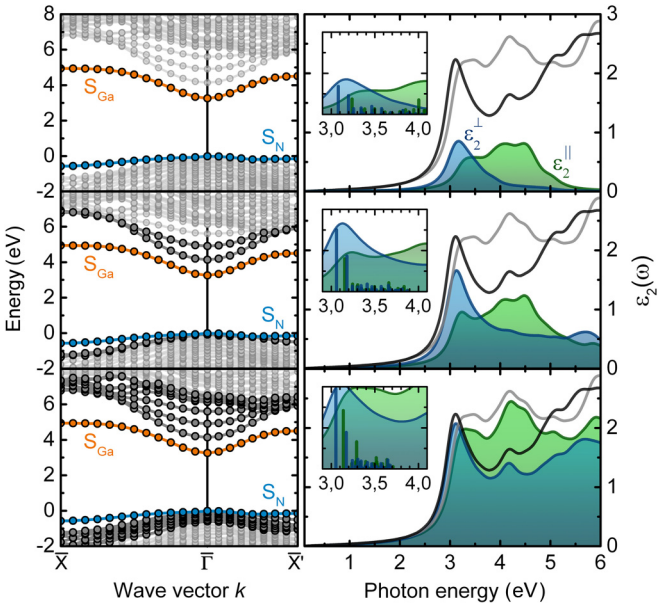

FIG. 8. (Color online) Illustration of the energy-band dependence of the GaN m-plane optical response. The panels on the right-hand side visualize the particular polarization-dependent contributions from the various surface-surface, surface-bulk, and bulk-bulk transitions to the surface optical response that stem from the bands indicated in full color on the left-hand side. Electron bands shown in translucent color where neglected in the respective calculations. Also shown on the right-hand side are the lowest eigenvalues of the BSE and their oscillator strength scaled by a factor of 10. Gray and black lines represent the total polarization-dependent dielectric functions of the GaN surface slab.

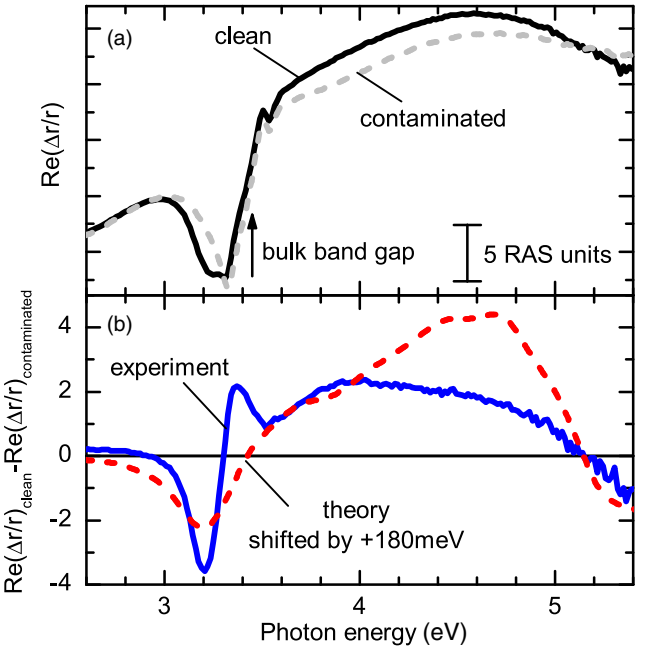

FIG. 9. (Color online) Optical anisotropy of m-plane GaN. (a) Experimental spectra of clean and contaminated GaN (see also Ref. [10]). (b) Difference of the two experimental RAS spectra obtained on the clean and contaminated surface (solid blue line) as well as the difference of the calculated RAS spectra of bulk plus surface and bulk, using the dielectric functions from Figs. 7 and 8.

In the present study, the spectral range of the RAS experiments is extended to higher energies in order to cover all interband transitions within the surface band structure. In the upper panel of Fig. 9, the optical anisotropy spectra of the clean and adsorption modified m-plane GaN surface are shown in the spectral range from 2.4 to 5.4 eV. In the lower panel, the difference between the spectra of clean and adsorption modified m-plane samples is plotted. The difference should be related to the surface optical anisotropy, assuming that the bulk anisotropy remains unaffected by surface contamination. For a more quantitative comparison between the measured data and the present calculations, we model the optical anisotropy on the basis of the calculated dielectric functions within the three-layer optical model. Thereby, we describe the system by a surface layer on top of the optically anisotropic GaN bulk material. The result, based on the respective calculated slab and bulk dielectric functions shown in Fig. 7, is given in the bottom panel of Fig. 9. The overall agreement between calculation and experiment is evident. The deviations between the measured and simulated amplitudes are not too surprising: On the one hand, the surface states might not be fully quenched by the residual gas absorption, and finite-temperature effects as well as sample inhomogeneities are not considered in the calculation. On the other hand, the three-layer model itself is an approximation and the accuracy of the calculated bulk and slab dielectric functions suffers from the limited number of electron states that can be included in the solution of the Bethe-Salpeter equation. Still, the contribution of the surface states to the optical anisotropy is very clearly visible both in experiment and simulation. It gives rise to a narrow negative feature below the band gap (due to the onset of $\varepsilon_2^{\perp}$) followed by a broad positive band above the fundamental band gap (due to $\varepsilon_2^{\parallel}$).

IV. SUMMARY AND CONCLUSION

First-principles calculations on the structural properties, electronic bands, and optical response of the GaN m-plane have been performed and compared to the surface optical anisotropy of GaN. Our results show that the surface is characterized by a charge transfer from the surface Ga to the more electronegative surface N atom. This charge transfer results in a rehybridization of the surface atoms that causes a buckling of about 8° of the surface atoms, where the Ga atoms move into the surface. The filled N-derived p-like surface state is resonant with the bulk VBM at the origin of the Brillouin zone. The empty Ga-derived p-like surface state, on the other hand, is well separated from the bulk CBM by at least 0.2 eV within the whole Brillouin zone and this gives rise to an intrinsic pinning of the Fermi level at the GaN m-plane. Both surface states contribute to the surface optical response and its anisotropy. The optical anisotropy shows strong and distinct contributions related to the N and Ga dangling-bond-derived surface bands, starting below the fundamental band gap up to approximately 5 eV. Our calculations show that the onset of the optical absorption of the GaN m-plane is defined by surface excitons which intermix contributions of the two surface states and near-band-edge electronic bands of the bulk.

ACKNOWLEDGMENTS

The numerical calculations were done using grants of computer time from the Regionales Rechenzentrum of the Universität zu Köln (RRZK), the Paderborn Center for Parallel Computing (PC^2), and the Höchstleistungs-Rechenzentrum Stuttgart (HLRS). The Deutsche Forschungsgemeinschaft (DFG) is acknowledged for financial support (Grants No. TRR142 and No. GRK1464). M. Himmerlich and S. Krischok are gratefully acknowledged for help with the experimental surface preparation.

[1] S. Nakamura, T. Mukai, and M. Senoh, Appl. Phys. Lett. **64**, 1687 (1994).

[2] F. Bernardini, V. Fiorentini, and D. Vanderbilt, Phys. Rev. B **56**, R10024 (1997).

[3] P. Waltereit, O. Brandt, A. Trampert, H. Grahn, J. Menniger, M. Ramsteiner, M. Reiche, and K. Ploog, Nature (London) **406**, 865 (2000).

[4] J. E. Northrup and J. Neugebauer, Phys. Rev. B **53**, R10477 (1996).

[5] D. Segev and C. G. Van de Walle, Europhys. Lett. **76**, 305 (2006).

[6] C. G. Van de Walle and D. Segev, J. Appl. Phys. **101**, 081704 (2007).

[7] M. Bertelli, P. Löptien, M. Wenderoth, A. Rizzi, R. G. Ulbrich, M. C. Righi, A. Ferretti, L. Martin-Samos, C. M. Bertoni, and A. Catellani, Phys. Rev. B **80**, 115324 (2009).

[8] L. Lymperakis, P. H. Weidlich, H. Eisele, M. Schnedler, J.-P. Nys, B. Grandidier, D. Stivenard, R. E. Dunin-Borkowski, J. Neugebauer, and P. Ebert, Appl. Phys. Lett. **103**, 152101 (2013).

[9] L. Ivanova, S. Borisova, H. Eisele, M. Dähne, A. Laubsch, and P. Ebert, Appl. Phys. Lett. **93**, 192110 (2008).

[10] M. Himmerlich, A. Eisenhardt, S. Shokhovets, S. Krischok, J. Räthel, E. Speiser, M. D. Neumann, A. Navarro-Quezada, and N. Esser, Appl. Phys. Lett. **104**, 171602 (2014).

[11] J. P. Perdew, K. Burke, and M. Ernzerhof, Phys. Rev. Lett. **77**, 3865 (1996).

[12] J. Heyd, G. E. Scuseria, and M. Ernzerhof, J. Chem. Phys. **118**, 8207 (2003).

[13] M. Landmann, E. Rauls, W. G. Schmidt, M. Röppischer, C. Cobet, N. Esser, T. Schupp, D. J. As, M. Feneberg, and R. Goldhahn, Phys. Rev. B **87**, 195210 (2013).

[14] L. G. Ferreira, M. Marques, and L. K. Teles, Phys. Rev. B **78**, 125116 (2008).

[15] F. Bechstedt, *Festkörperprobleme/Advances in Solid State Physics* (Vieweg, Braunschweig/Wiesbaden, 1992), Vol. 32, p. 161.

[16] G. Kresse and D. Joubert, Phys. Rev. B **59**, 1758 (1999).

[17] G. Kresse and J. Furthmüller, Comput. Mater. Sci. **6**, 15 (1996).

[18] I. Vurgaftman and J. R. Meyer, J. Appl. Phys. **94**, 3675 (2003).

[19] J. Heyd, J. E. Peralta, G. E. Scuseria, and R. L. Martin, J. Chem. Phys. **123**, 174101 (2005).

[20] S. Albrecht, L. Reining, R. DelSole, and G. Onida, Phys. Rev. Lett. **80**, 4510 (1998).

[21] L. X. Benedict, E. L. Shirley, and R. B. Bohn, Phys. Rev. Lett. **80**, 4514 (1998).

[22] M. Rohlfing and S. G. Louie, Phys. Rev. Lett. **83**, 856 (1999).

[23] W. G. Schmidt, S. Glutsch, P. H. Hahn, and F. Bechstedt, Phys. Rev. B **67**, 085307 (2003).

[24] P. H. Hahn, W. G. Schmidt, and F. Bechstedt, Phys. Rev. Lett. **88**, 016402 (2001).

[25] F. Fuchs, C. Rödl, A. Schleife, and F. Bechstedt, Phys. Rev. B **78**, 085103 (2008).

[26] N. Esser, W. G. Schmidt, C. Cobet, K. Fleischer, A. I. Shkrebtii, B. O. Fimland, and W. Richter, J. Vac. Sci. Technol. B **19**, 1756 (2001).

[27] K. Hingerl, D. E. Aspnes, I. Kamiya, and L. T. Florez, Appl. Phys. Lett. **63**, 885 (1993).

[28] R. Azzam and N. Bashara, *Ellipsometry and Polarized Light*, 3rd ed. (North-Holland, Amsterdam, 1996).

[29] José Luiz A. Alves, J. Hebenstreit, and M. Scheffler, Phys. Rev. B **44**, 6188 (1991).

[30] J. Hebenstreit, M. Heinemann, and M. Scheffler, Phys. Rev. Lett. **67**, 1031 (1991).

[31] M. D. Pashley, Phys. Rev. B **40**, 10481 (1989).

[32] W. G. Schmidt, Appl. Phys. A **65**, 581 (1997).

[33] W. G. Schmidt, Appl. Phys. A **75**, 89 (2002).

[34] W. G. Schmidt, F. Bechstedt, and G. P. Srivastava, Surf. Sci. Rep. **25**, 141 (1996).

[35] M. Feneberg, M. F. Romero, M. Röppischer, C. Cobet, N. Esser, B. Neuschl, K. Thonke, M. Bickermann, and R. Goldhahn, Phys. Rev. B **87**, 235209 (2013).

[36] R. Laskowski, N. E. Christensen, G. Santi, and C. Ambrosch-Draxl, Phys. Rev. B **72**, 035204 (2005).

[37] L. C. de Carvalho, A. Schleife, J. Furthmüller, and F. Bechstedt, Phys. Rev. B **87**, 195211 (2013).